

COMPOSITIONAL MAPPING OF VESTA QUADRANGLE V24. F. Tosi¹, M.C. De Sanctis¹, A. Nathues², E. Ammannito¹, A. Frigeri¹, F. Zambon¹, E. Palomba¹, F. Capaccioni¹, A. Yingst³, R. Jaumann⁴, K. Stephan⁴, C.M. Pieters⁵, C.A. Raymond⁶, C.T. Russell⁷, and the Dawn Team. ¹INAF-IAPS, Via del Fosso del Cavaliere 100, I-00133 Rome, Italy, federico.tosi@ifsi-roma.inaf.it. ²Max Planck Institute for Solar System Research, Max-Planck-Strasse 2, D-37191 Katlenburg-Lindau, Germany. ³Planetary Science Institute, 1700 East Fort Lowell, Tucson, AZ 85719-2395, USA. ⁴Institute of Planetary Research, German Aerospace Center (DLR), Rutherfordstrasse 2, D-12489 Berlin, Germany. ⁵Department of Geological Sciences, Brown University, 324 Brook Street, Providence, RI 02912, USA. ⁶NASA/Jet Propulsion Laboratory and California Institute of Technology, 4800 Oak Grove Drive, Pasadena, CA 91109, USA. ⁷Institute of Geophysics and Planetary Physics, University of California at Los Angeles, 3845 Slichter Hall, 603 Charles E. Young Drive, East, Los Angeles, CA 90095-1567, USA.

Introduction: The Dawn spacecraft [1] entered orbit around Vesta in mid-July 2011. Since then, the Visible and InfraRed Imaging Spectrometer (VIR) [2] acquired hyperspectral images of Vesta's surface in the overall wavelength range from 0.25 to 5.1 μm .

During the Approach and Survey mission phases (23 July through 29 August 2011), VIR obtained resolved images of Vesta with spatial resolutions between 1.31 km and 0.68 km/pix. More than 65% of the surface, from the South Pole up to $\sim 40^\circ\text{N}$, was observed under different illumination conditions and local solar elevations.

Based on this datasets, a series of four quadrangle maps following the scheme in [3] are being produced showing the results derived from the spectroscopic analysis of VIR data. In this work we present the results of the spectroscopic analysis achieved for the quadrangle V-24, which covers Vesta's southern polar region $55^\circ\text{S} - 90^\circ\text{S}$ and longitude $0^\circ - 360^\circ$.

Major spectral properties: 4 Vesta is known to have a surface of basaltic material through visible/near-infrared reflectance spectroscopy [4]. Vesta's spectrum has strong absorption features centered near 0.9 and 1.9 μm (hereafter labeled as BI and BII), indicative of Fe-bearing pyroxenes [5]. The spectra of the howardite, eucrite and diogenite (HED) meteorites clan have similar features [4], which led to the hypothesis that Vesta is the parent body of the HED clan [6,7]. Although pyroxenes' signatures are ubiquitous on Vesta and largely dominate its surface composition, significant variability in slope, strength and wavelength position of the center of these signatures can be measured, which indicate multiple physical surface processes [5].

On the basis of several spectral indices, the surface of Vesta as imaged by VIR can be divided into different terrain types [5], which are mostly related to specific geological units or morphological surface features. Different surface materials are enhanced by combining different spectral channels or band ratios into color images and are known to be sensitive to the content of mafic minerals in the surface material as well as its relative freshness [8].

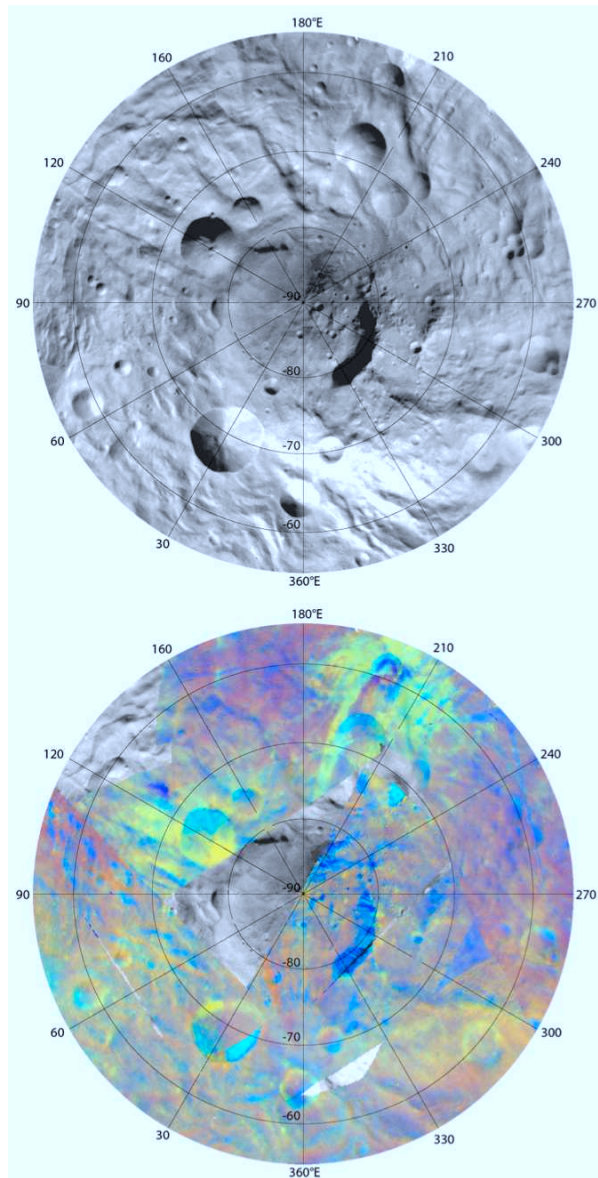


Figure 1. Upper panel: Mosaic of Dawn's Framing Camera (FC) data representing Vesta's quadrangle V-24 (southern polar region of up to 55°S). Data were acquired during the Survey phase with the clear filter, and were corrected here with a Hapke photometric function. **Lower panel:** RGB composite of the same region made from VIR color ratios: $R = 438\text{nm}/749\text{nm}$, $G = 749\text{nm}/917\text{nm}$, $B = 749\text{nm}/438\text{nm}$

(“Clementine” colors), superimposed to the optical mosaic. Color ratios may enhance differences in material and composition and shed light on the lithology.

As a first step, we made a RGB composite of the southern polar region by using VIR color ratios at 438nm/749nm, 749nm/917nm and 749nm/438nm respectively (so-called “Clementine” color code). Combined with the visible albedo of Vesta’s surface, this color-ratio composite shows: 1) bright material in yellow/green, 2) dark material in blue/violet, and 3) spectrally distinct ejecta in red/purple (**Fig. 1**).

The southern region of Vesta is dominated by the largest impact structure of the asteroid, the 500-km Rheasilvia basin, which excavated deep into the crust [9]. VIR spectral data indicate that this lower crustal material appears to have particular spectral characteristics, represented by the so-called *southern terrains (ST)* which dominate this part of the asteroid [5]. They generally show deeper and wider band depths and average band centers at shorter wavelengths, a spectral behavior which indicates the presence of Mg-pyroxene-rich terrains in Rheasilvia.

Results: The southern polar region is characterized by a greater abundance of bright materials, often associated with strong pyroxenes bands. However, the “yellow/green” signature as inferred from the above color ratios clearly shows an asymmetric trend across this region. In addition, bright relatively fresh material can also be observed at local scale, e.g. in some parts of the scarp of the Rheasilvia basin (see **Fig. 2**), as well as on crater walls of impact craters with pronounced topography where fresh material became exposed due to mass wasting processes.

To deepen our understanding of Vesta’s surface composition, besides color ratios, other spectral indices must be considered. BI depths in the Rheasilvia basin commonly are significantly larger than in the equatorial region. Similarly, BII depths in the southern region have values 1.5-1.7 times greater than those found in the equatorial region. The depth of an absorption band is mainly determined by the abundance of the absorbing minerals, the grain size distribution of the soil, and the presence of opaques. VIR data suggest that the region of the Rheasilvia basin is richer in pyroxene than the equatorial regions of Vesta or that the regolith in this region has a larger grain size distribution and/or fewer opaques (or a combination of the two causes).

Maps of the BII centers show that in the southern polar region they are at generally shorter wavelengths than in the equatorial region, and that the global variation in BII centers often corresponds closely to, but inversely with, band depth variations: for example, in the Rheasilvia basin, the BII centers are at shorter

wavelengths and these often correspond to the deepest pyroxene absorption bands.

The correspondence of stronger pyroxene absorption with lower BII (and BI) centers in the Rheasilvia basin indicates a lithology dominated by the materials exposed on the surface, while terrains located at lower latitudes generally show a lithology marked by craters’ ejecta.

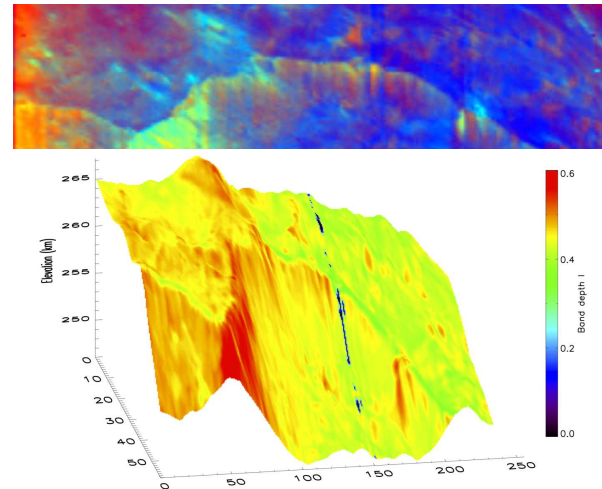


Figure 2. Upper panel: VIR cube showing a portion of the Rheasilvia basin’s scarp. This image has been elaborated by using the three color ratios: 438nm/749nm, 749nm/917nm and 749nm/438nm, in order to enhance differences in material and composition. In this way it is possible to identify three different classes of material (green, red and blue) that may correspond to different compositions, different ages or different structural properties (i.e., grain sizes of the regolith that covers the surface of the asteroid). **Lower panel:** Depth of pyroxene’s band at 0.9 μm in the same region highlighted by the upper panel. The information relative to the surface elevation can be added to provide clues to surface composition.

Acknowledgements: The authors acknowledge the support of the Dawn Science, Instrument and Operations Teams. This work was supported by the Italian Space Agency (ASI), ASI-INAF Contract I/026/05/0.

References:

- [1] Russell, C.T. et al. (2004) *PSS*, 52, 465–489.
- [2] De Sanctis, M.C. et al. (2011) *SSR*, 163.
- [3] Greeley, R. and Batson, G. (1990) *Planetary Mapping*, 32.
- [4] McCord T.B. et al. (1970) *Science* 168, 1445-1447.
- [5] De Sanctis, M.C. et al. (2012), LPS XLIII, this conference.
- [6] Consolmagno (1979).
- [7] Consolmagno and Drake (1977).
- [8] Tompkins, S. & Pieters, C.M. (1999) *Meteor. & Plan. Sc.*, 34, 25-41.
- [9] Schenk, P., et al. (2012), LPS XLIII, this conference.